Check for updates

Geophysical Research Letters

RESEARCH LETTER
10.1029/2021GL097089

Fewer Troughs, Not More Ridges, Have Led to a Drying Trend in the Western United States

Wei Zhang[1], Vittal Hari[2], Simon S-Y Wang[1,3], Matthew D. LaPlante[1,4], Gregg Garfin[5], Grace Affram[1], and Rohini Kumar[2]

[1]Department of Plants, Soils and Climate, Utah State University, Logan, UT, USA, [2]UFZ-Helmholtz Centre for Environmental Research, Leipzig, Germany, [3]Utah Climate Center, Utah State University, Logan, UT, USA, [4]Department of Journalism and Communication, Utah State University, Logan, UT, USA, [5]School of Natural Resources and the Environment, University of Arizona, Tucson, AZ, USA

Key Points:

- No discernable trend is evident for dry- and warm-weather-inducing ridge conditions
- Trough conditions-the largest contributor to annual precipitation in the western U.S.-have undergone a distinctive decrease in frequency
- The decreasing trend in western troughs is likely to have occurred in response to external forcing rather than natural forcing alone

Supporting Information:

Supporting Information may be found in the online version of this article.

Correspondence to:

W. Zhang,
w.zhang@usu.edu

Citation:

Zhang, W., Hari, V., S-Y Wang, S., LaPlante, M. D., Garfin, G., Affram, G., & Kumar, R. (2022). Fewer troughs, not more ridges, have led to a drying trend in the western United States. *Geophysical Research Letters*, *49*, e2021GL097089. https://doi.org/10.1029/2021GL097089

Received 16 NOV 2021
Accepted 22 DEC 2021

Author Contributions:

Conceptualization: Wei Zhang
Formal analysis: Wei Zhang, Grace Affram
Funding acquisition: Wei Zhang
Investigation: Wei Zhang
Methodology: Wei Zhang, Vittal Hari, Simon S-Y Wang, Rohini Kumar
Validation: Wei Zhang
Writing – original draft: Wei Zhang
Writing – review & editing: Wei Zhang, Vittal Hari, Simon S-Y Wang, Matthew D. LaPlante, Gregg Garfin, Rohini Kumar

© 2021. American Geophysical Union. All Rights Reserved.

Abstract High-amplitude ridges can enforce heat-trapping systems that persist through an entire season, contributing to drought events. However, the impacts of day-to-day weather system changes at the meso- and synoptic-scale are also important, albeit less well studied. We identify five weather types (WTs) from 500-hPa geopotential height anomalies. These categories include WT4, which represents ridges and associated dry and warm anomalies, and WT3, which characterizes troughs and associated wetter- and colder-than-normal conditions and is the largest contributor to precipitation in the western U.S. While no discernable trend is evident for WT4 conditions, WT3 conditions have undergone a distinctive decrease in frequency at both annual and seasonal scales, thus a general drying trend across the west during this time period may be more significantly associated with fewer troughs rather than more ridges. Attribution analysis reveals that this decrease in wetter and colder weather is a likely result of anthropogenic forcing.

Plain Language Summary While it is well known that large, persistent areas of high pressure can trap heat in a region for an entire season, contributing to droughts, the impacts of day-to-day weather system changes at smaller scales have remained less studied. In this study, we learned that dry- and hot-weather-inducing ridge conditions did not significantly change during a period of generalized drying between 1980 and 2018. What did change during those years was the pattern of troughs, which are associated with wetter- and colder-than-normal conditions; these conditions became less common during those years. This trend is likely to have occurred in response to human-caused factors.

1. Introduction

The western United States is enduring a prolonged and intense drought, dubbed by a "megadrought," with historically destructive impacts on ecological and agricultural systems (E. R. Cook et al., 2004; Diffenbaugh et al., 2015; Piechota et al., 2004; Seager et al., 2015; Stahle, 2020; Svoboda et al., 2002; Williams et al., 2020). Associated with quasi-stationary atmospheric patterns (Swain, 2015; Swain et al., 2016; Teng & Branstator, 2017; Wang et al., 2017), the influence of anthropogenic forcing has unequivocally increased the likelihood of drought (Delworth et al., 2015; Diffenbaugh et al., 2015; Mann & Gleick, 2015; Williams et al., 2015), and the most reliable climate models uniformly project an unprecedented increase in drought risk during the 21st century (Ault et al., 2016; Cook et al., 2015; Diffenbaugh et al., 2015; Mann & Gleick, 2015).

Persistent high-pressure ridges in the upper troposphere (Hartmann, 2015; Lund et al., 2018; Seager et al., 2015; Swain et al., 2014, 2016; Swain, 2015; Williams et al., 2015), such as the amplified anticyclones that played a crucial role in the drought of 2014–2015 (Swain, 2015; Swain et al., 2016; Teng & Branstator, 2017; Wang et al., 2014, 2017), drive increased temperatures while reducing rainy-season precipitation (Singh et al., 2016), resulting in heating and drying trends (Figure 1a). Likewise, persistent West Coast trough anomalies during the flipped phase of the standing wave pattern induce wet and cold conditions, including flooding (Wang et al., 2017). While it might seem intuitive that a standing wave pattern represents a balanced relationship of ridges and troughs, the transient and episodic nature of troughs is, in fact, distinct from the lingering and quasi-stationary tendency of ridges, and it is the dynamic, shorter-term frequency of troughs that yields the greatest share of precipitation during the rainy season in the western United States (Gillies et al., 2010; Wang et al., 2012).

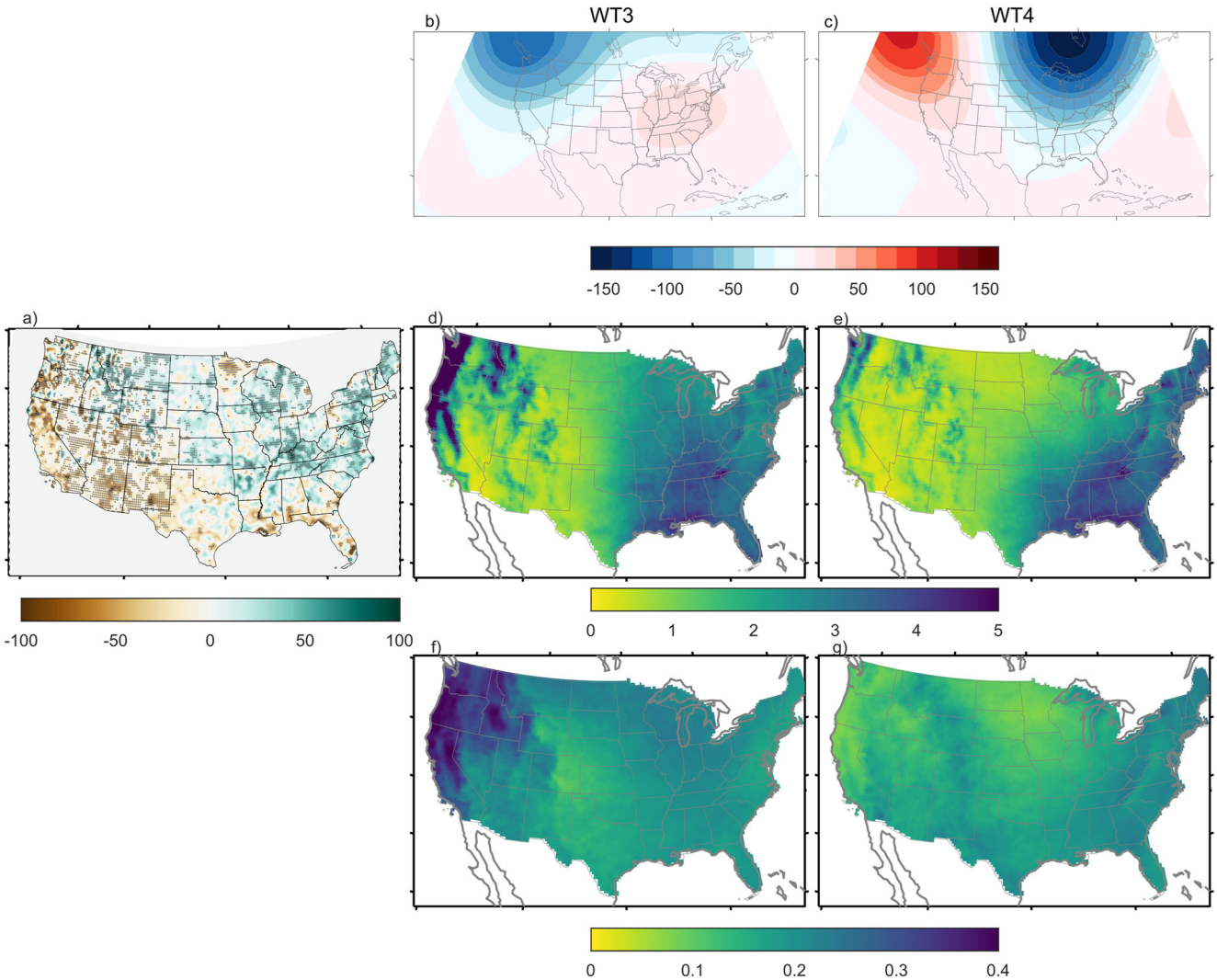

Figure 1. (a) Trend in annual total precipitation (shading: unit: mm/decade) over the continental US during 1980–2018. The hatched regions are statistically significant at the 0.05 level. (b) 500-hPa geopotential height anomaly (unit: gpm), (d) composite precipitation (unit: mm/day) and (f) fractional contribution of WT3 (the western trough pattern) precipitation to total precipitation. (c) 500-hPa geopotential height anomaly, (e) composite precipitation and (g) precipitation fraction for WT4 (the western ridge pattern).

While the strength of the seasonal-mean atmospheric ridge has increased, as previously documented (Diffenbaugh et al., 2015; Swain, 2015; Wang et al., 2017; Yoon et al., 2015), the impact of day-to-day weather system changes at the meso- and synoptic-scale on drought events are not yet clear. Here, we examine the day-to-day ridge and trough patterns from the perspective of weather types within a transient framework.

2. Data and Methods

Daily precipitation data over the continental United States is obtained from the Climate Prediction Center at 0.25 spatial resolution (Chen et al., 2008). The 500-hPa geopotential height data for deriving the weather types/regimes are obtained from the National Aeronautics and Space Administration (NASA)'s Modern-Era Retrospective Analysis for Research and Applications, version 2 (MERRA-2) at 0.5° × 0.625° spatial resolution for 1980-present (Gelaro et al., 2017); the European Center for Medium-Range Weather Forecasts (ECMWF)'s ERA-5 at 0.25° × 0.25° spatial resolution (1979-present; Hersbach et al., 2020); the National Centers for Environmental Prediction and National Center for Atmospheric Research (NCEP/NCAR) reanalysis data at 2.5° × 2.5° spatial resolution (1948-present; Kalnay et al., 1996); and the Japanese 55-year ReAnalysis (JRA-55, 1958-present) at

19448007, 2022, 1, Downloaded from https://agupubs.onlinelibrary.wiley.com/doi/10.1029/2021GL097089 by Office Of Scientific And Technical Information, Wiley Online Library on [28/07/2023]. See the Terms and Conditions (https://onlinelibrary.wiley.com/terms-and-conditions) on Wiley Online Library for rules of use; OA articles are governed by the applicable Creative Commons License

19448007, 2022, 1, Downloaded from https://agupubs.onlinelibrary.wiley.com/doi/10.1029/2021GL097089 by Office Of Scientific And Technical Information, Wiley Online Library on [28/07/2023]. See the Terms and Conditions (https://onlinelibrary.wiley.com/terms-and-conditions) on Wiley Online Library for rules of use; OA articles are governed by the applicable Creative Commons License

1.25° × 1.25° spatial resolution (Kobayashi et al., 2015). The daily temperature data set is obtained from Berkeley Earth (http://berkeleyearth.org/data/; Rohde et al., 2011). We use daily 500-hPa geopotential height data from the Coupled Model Intercomparison Project Phase 6 (CMIP6) project (Eyring et al., 2016; Table S1 in Supporting Information S1) and CESM large ensemble run with 42 members (Kay et al., 2015). We use four models in CMIP6 with all the experiments (Hist_All, Hist_GHG, and Hist_NAT) and variables (daily 500-hPa geopotential height) available (Eyring et al., 2016). To examine the internal variability of the trends in weather types, we examine the trends over 39-year moving windows in the Preindustrial (PI) control run in CMIP6. The k-means cluster analysis (refer to Text S1 in Supporting Information S1) is used to identify weather types/regimes from the daily 500-hPa geopotential height anomalies, based on the period from 1980 to 2010, over the continental U.S. similar to previous works (Zhang & Villarini, 2019, 2021). No temporal smoothing or filtering has been applied to the daily 500-hPa geopotential height anomaly. Although our focus is on understanding precipitation trends in the western U.S., we use daily 500-hPa geopotential height anomalies over the full continental U.S. to identify the weather types because a broader picture of large-scale circulations can better explain precipitation variability in the study region (Robertson & Ghil, 1999; Steinschneider et al., 2019).

3. Results

Following previous studies that examine weather types (WT; Zhang & Villarini, 2019, 2021; Methods; Figure S1; left panels), we apply K-means clustering to daily 500-hPa geopotential height anomalies based on reanalysis data, resulting in five distinct WT over the continental United States. Each WT represents a unique, large-scale pattern that modulates precipitation and temperature on a day-to-day basis. Weather Type 3 (WT3) is associated with a deep trough in the western U.S. (Figure 1b), while WT4 represents a strong ridge pattern similar to the amplified and semi-permanent ridge associated with severe drought conditions in California (Hartmann, 2015; Seager et al., 2015; Swain, 2015; Swain et al., 2016; Williams et al., 2015; Figure 1c). In essence, WT3 is associated with low atmospheric pressure and strong moisture flux transported to the western U.S. while WT4 is associated with high atmospheric pressure and weak moisture flux transported to this region (Figure S1 in Supporting Information S1; right panels). It bears noting, however, that WT3 and WT4 are not mirror opposites. Previous studies have identified general weather regimes and those related to ridge patterns in the western U.S. For example, Gibson et al. (2020) identified four ridge types in the western U.S. using empirical orthogonal function (EOF) analysis. Among these four ridge types, ridge type 1 (N-ridge) is similar to WT4 of the present study. In addition, Vigaud et al. (2018) found four weather regimes over North America from October to March, with their weather regime 1/4 being similar to WT4/3 of the present study. While Gibson et al. (2020) cautioned that the seasonal changes in ridge patterns over the western U.S. could be significant, we found that seasonal differences in the geopotential height anomaly for each weather type are generally small (Figure S2 in Supporting Information S1). The exception is WT3 which, during June-August, is more greatly divergent from the other seasons.

Five WTs exhibit distinct characteristics of composite precipitation and fractional contribution in the western U.S. (Figure S3 in Supporting Information S1) and this is also true across different seasons (Figures S4 and S5 in Supporting Information S1). WT3 exhibits higher precipitation and fractional precipitation contribution than WT4 (Figures 1d–1g), as well as colder temperatures (Figure S6 in Supporting Information S1), an effect that is particularly pronounced in the winter season, which is similar to the Central and Midwestern regions of the U.S. (Zhang & Villarini, 2019, 2021).

Using Poisson regression (Cameron & Trivedi, 2013; see Methods), we detect a significant decreasing trend (Beta $= -0.0147$, p-value < 0.01) in the annual frequency of WT3 from 1980 to 2018 that is consistent across different reanalysis data sets (Figure S7 in Supporting Information S1). No such trend can be detected for WT4 (Figure 2). The results are consistent at the seasonal scale, exhibiting significant decreasing trends for WT3 and insignificant trend for WT4 during March-May (MAM), June-August (JJA), September-November (SON) and December-February (DJF; Figure S8 in Supporting Information S1). Assessing the relative roles of the different weather types in shaping the change of annual total precipitation, we see the decrease in WT3-associated precipitation has a magnitude and pattern (Figure 2) similar to that of the annual total precipitation declines from 1980 to 2018 (Figure 1a) while the change in WT4 exhibits a much weaker and insignificant trend.

Next, we use CMIP6 experiments (see Methods) to evaluate the possible roles of external forcing (including greenhouse gas and natural forcing) on the decreasing frequency of WT3. When only natural forcings are

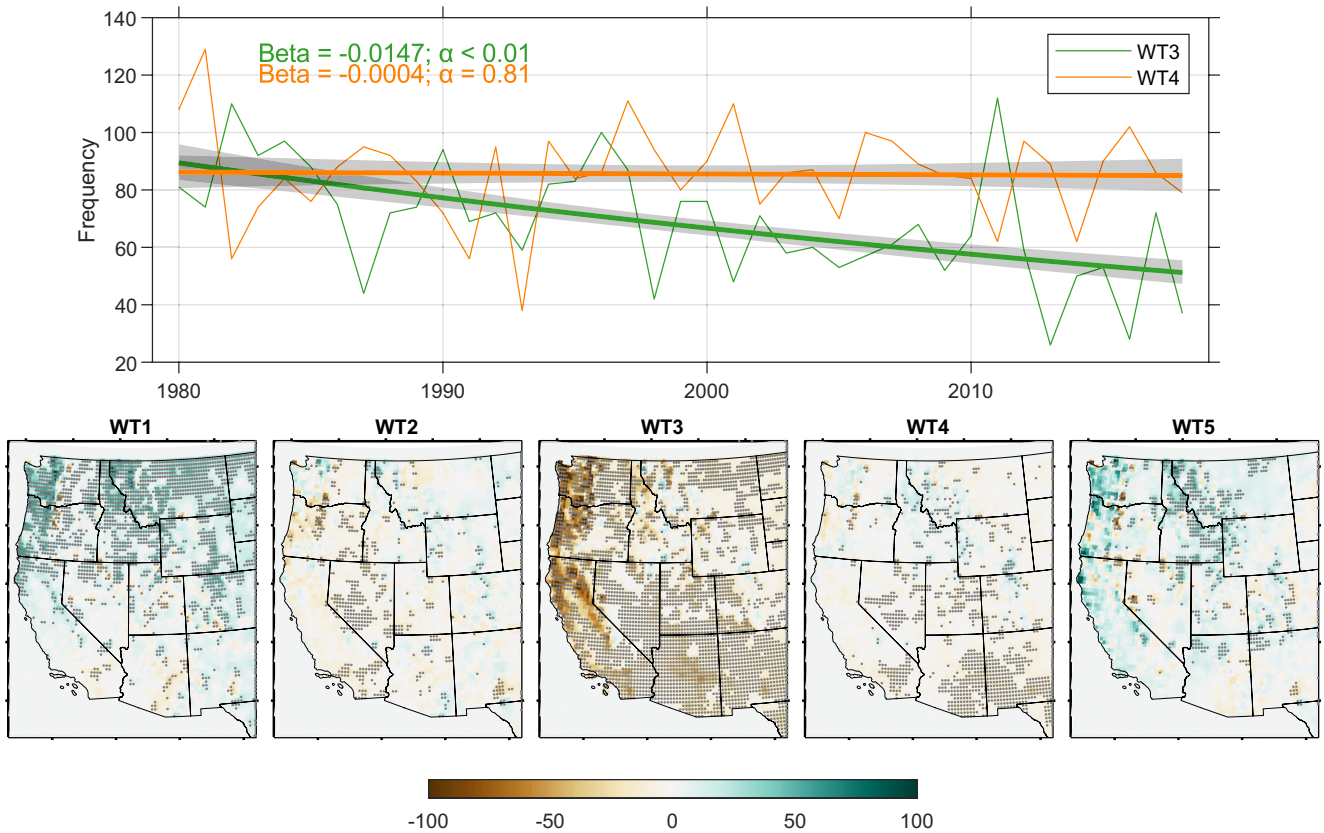

Figure 2. Top: Frequencies (unit: events) and fitted trends (unit: events/yr) for weather types 3 and 4 during 1980–2018. Bottom: precipitation trend (unit: mm/decade) in the western US associated with WT1-5. The shading in the top panel represents the 95% confidence interval of the fitted trend using Poisson regression. The hatched regions are statistically significant at the 0.05 level.

prescribed in the experiments, the frequency of WT3 does not reveal any significant change (Figure 3a), while in experiments that include all historical forcings (i.e., greenhouse gases and natural forcings) or greenhouse gases, we find similar decreasing trends in the frequency of WT3–this is observed in all historical forcings (Beta = −0.0121; p-value < 0.01; Figure 3a) and greenhouse-gas forcings (Beta = −0.007; p-value < 0.01; Figure 3a), which echoes what was revealed in reanalysis data (Beta = −0.0147; p-value < 0.01; Figure 2). The probability distributions of the trends (i.e., Poisson regression slope) for each model member further support the above results (Figure 3a). These findings align to large ensemble runs performed using the National Center for Atmospheric Research (NCAR)'s Community Earth System Model (CESM) (*28*), showing a consistent decreasing trend (Beta = −0.003; p-value < 0.05) in WT3 under prescribed external forcing from 1948 to 2005, which is supported by the probability distribution of the trends (Figure 3b). The results thus offer further evidence that the decreasing trend in WT3 can be attributed to contemporary anthropogenic greenhouse gas emissions. The decreasing trend in WT3 is consistent when we extended the period to 1920–2005 (Beta = −0.002; p-value < 0.05; Figure S9 in Supporting Information S1). By contrast, no significant trend is revealed in the frequency of WT4 under a similar analysis, regardless of the external forcings.

To understand the mechanisms underlying the changes in WT3 and WT4, we computed the mean ridge index based on 250-hPa geopotential height averaged over the domain (135°W–120°W, 30°N–50°N), following Yoon et al. (2015), which studied the driver of water cycle extremes in the western U.S. Under this analysis, the ridge index exhibits a significant upward trend during the period of November-April of 1980–2018 (Figure S10 in Supporting Information S1; beta = 1.0427 gpm/yr; p-value < 0.05). While this trend in the mean western ridge is known, the significant negative correlations between the monthly ridge index and the monthly frequency of WT3 (Figure S11 in Supporting Information S1; detrended) represent a previously unknown feature. The monthly frequency of WT4, meanwhile, has an insignificant positive correlation with the monthly ridge index (Figure S10 in Supporting Information S1), suggesting that the transient ridge system simply reflects the mean state of the

19448007, 2022, 1, Downloaded from https://agupubs.onlinelibrary.wiley.com/doi/10.1029/2021GL097089 by Office Of Scientific And Technical Information, Wiley Online Library on [28/07/2023]. See the Terms and Conditions (https://onlinelibrary.wiley.com/terms-and-conditions) on Wiley Online Library for rules of use; OA articles are governed by the applicable Creative Commons License

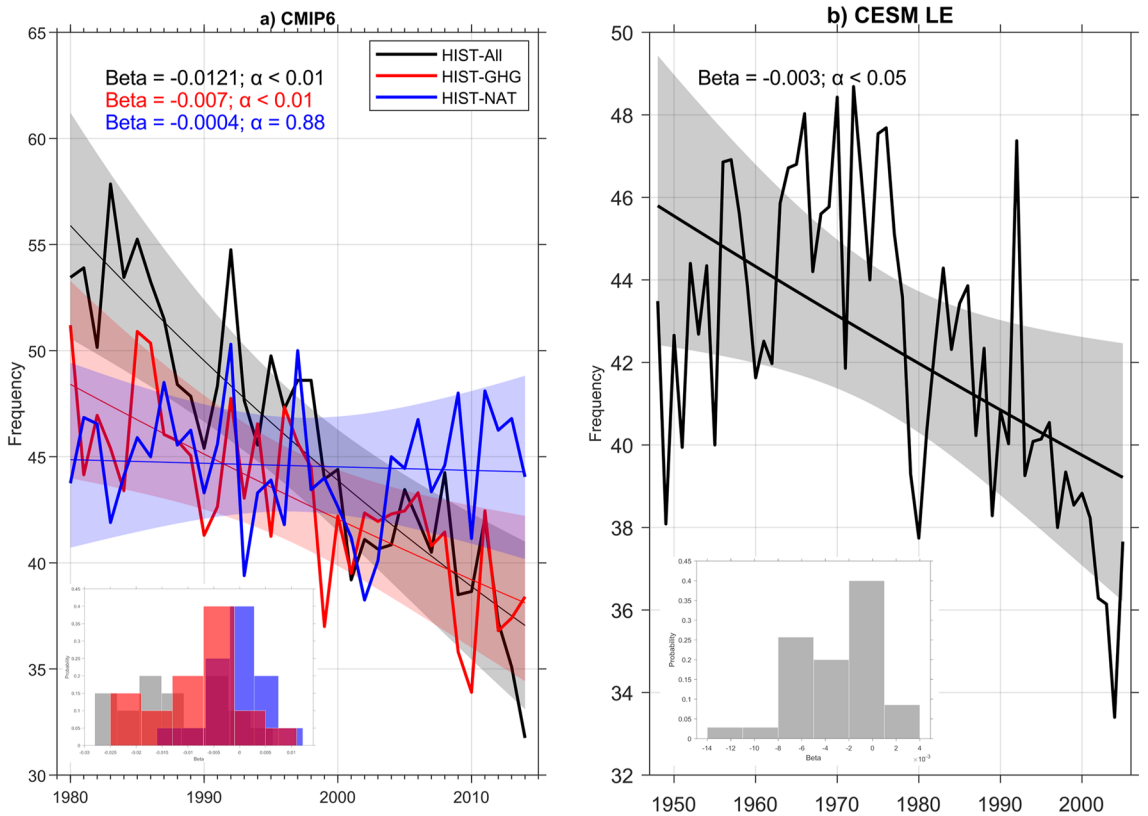

Figure 3. (a) Frequencies (events) and trends of WT3 (events/year) during 1980–2014 based on HIST-All (black), HIST-GHG (red), and HIST-NAT (blue) experiments using CMIP6 model data. The panel in the bottom shows the probability distribution of regression slope (WT3) in CMIP6 HIST-All and HIST-NAT experiments. (b) Frequencies and trends of WT3 during 1950–2004 based on HIST-All CESM large ensemble run. The panel in the bottom shows the probability distribution of regression slope (WT3) in HIST-All CESM experiments. The shading buffers show the 95th confidence interval of the trends.

background flow associated with the wintertime stationary waves over North America (Chien et al., 2019; Singh et al., 2016; Wang et al., 2017). This result lends further support to the hypothesis of a declining trend in WT3, suggesting blocking of transient trough systems (given its prominent negative correlation with the mean ridge index that has increased profoundly). While the weather types are obtained over the continental U.S., our method may miss some ridge patterns that are important for the precipitation in the western U.S. For example, Gibson et al. (2020) found that the southwestern U.S. ridge pattern exhibits a slight upward trend in frequency, which has contributed to the drying trend. However, this ridge pattern has not been found in this study, probably due to the broader domain we select for the K-means cluster analysis.

Previous studies have attributed the increasing trend in the mean ridge variability over the western U.S. to anthropogenic forcing (Swain et al., 2014; Wang et al., 2014), further supporting our modeling results (Figure 3). While we aim to understand the impacts of external forcing (e.g., anthropogenic forcing), it is also useful to examine the internal variability of WT3 in CMIP6 experiments that represents unforced climate variations (e.g., Deser et al., 2014; Kay et al., 2015). Using the preindustrial (Pi-control) experiments in CMIP6, we identify both downward and upward trends in WT3 during 39-year moving windows (Figure S12 in Supporting Information S1). However, the trend in WT3 averaged over all the 39-year moving windows is ~0 (Figure S12 in Supporting Information S1). Following Barkhordarian et al. (2013), the upward trends in WT3 during the 39-year moving windows of Pi-control experiments are used to test the null hypothesis that may be stated as "the trend of WT3 in the experiments with all historical forcings is equal to 0 (Beta = 0)." The trend of WT3 in all historical forcings is statistically significant at the 0.01 level using this framework (Barkhordarian et al., 2013). This indicates that external forcing (e.g., anthropogenic forcing), which overpowers internal variability, is mainly responsible for the observed decreasing trend in WT3.

19448007, 2022, 1, Downloaded from https://agupubs.onlinelibrary.wiley.com/doi/10.1029/2021GL097089 by Office Of Scientific And Technical Information, Wiley Online Library on [28/07/2023]. See the Terms and Conditions (https://onlinelibrary.wiley.com/terms-and-conditions) on Wiley Online Library for rules of use; OA articles are governed by the applicable Creative Commons License

19448007, 2022, 1, Downloaded from https://agupubs.onlinelibrary.wiley.com/doi/10.1029/2021GL097089 by Office Of Scientific And Technical Information, Wiley Online Library on [28/07/2023]. See the Terms and Conditions (https://onlinelibrary.wiley.com/terms-and-conditions) on Wiley Online Library for rules of use; OA articles are governed by the applicable Creative Commons License

To assess potential impacts of thermal expansion on the decreasing trend in WT3, we also performed an analysis by removing the seasonal mean hemispheric trend in the daily geopotential height anomalies, following previous studies (e.g., Horton et al., 2015; Swain et al., 2016, 2018). Overall, the WTs are consistent with the results without removing the seasonal mean hemisphere (Figure S13 in Supporting Information S1) and the significant decreasing trend in WT3 still exists for the annual total frequency of this weather type (Figure S14 in Supporting Information S1). This suggests that thermal expansion may play a possible secondary role in decreasing the frequency of WT3. Previous research has found that anthropogenic forcing tends to induce El Niño-like sea surface temperature (SST) patterns (Cai et al., 2021; Xie et al., 2010), which may reduce the occurrence of WT3. Notably, we find that a La Niña-like pattern is identified by regressing SST onto the detrended frequency of WT3 (Figure S15 in Supporting Information S1), indicating that a La Niña-like pattern is associated with more WT3 events.

4. Summary

While an amplified seasonal-mean ridge may play a partial role in explaining recent California droughts and warming, our analysis indicates that it is the decreasing trend in transient western troughs that has contributed the most to the downward trend in the annual and seasonal precipitation totals across the western U.S. These findings highlight the importance of improved understanding of time-mean features (i.e., stationary waves over North America) and transient weather patterns (e.g., cold fronts), their respective trends, and possible external forcings. Our study also points to the need to improve the underlying atmospheric and oceanic drivers of western U.S. drought to aid drought prediction.

Conflict of Interest

The authors declare no conflicts of interest relevant to this study.

Data Availability Statement

The CMIP6 model outputs were obtained from the website (https://esgf-node.llnl.gov/projects/cmip6/). The CMIP6 models used in the study are referenced in Table S1 in the Supporting Information S1. The CESM large ensemble runs were accessed via https://www.cesm.ucar.edu/projects/community-projects/LENS/data-sets.html. The daily temperature data set was obtained from Berkeley Earth (http://berkeleyearth.org/data/). The daily precipitation data was provided by NOAA Physical Sciences Laboratory (https://psl.noaa.gov/data/gridded/data.unified.daily.conus.html).

Acknowledgments
We thank the two anonymous reviewers for insightful comments that improve the quality of this manuscript. WZ is supported by USDA NIFA Hatch Project (1026229), the UAES Seed Grant, Utah Agricultural Experiment Station (approved as journal paper number #9549), the U.S. Department of Interior, Bureau of Reclamation and the startup fund of Utah State University. S.W. is supported by U.S. Department of Energy under Award Number DE-SC0016605 and by NSF P2C2 award number 1903721.

References

Ault, T. R., Mankin, J. S., Cook, B. I., & Smerdon, J. E. (2016). Relative impacts of mitigation, temperature, and precipitation on 21st-century megadrought risk in the American Southwest. *Science Advances*, *2*(10), e1600873. https://doi.org/10.1126/sciadv.1600873

Barkhordarian, A., von Storch, H., & Bhend, J. (2013). The expectation of future precipitation change over the Mediterranean region is different from what we observe. *Climate Dynamics*, *40*(1), 225–244. https://doi.org/10.1007/s00382-012-1497-7

Cai, W., Santoso, A., Collins, M., Dewitte, B., Karamperidou, C., Kug, J.-S., et al. (2021). Changing El Niño–southern oscillation in a warming climate. *Nature Reviews Earth & Environment*, *2*(9), 628–644. https://doi.org/10.1038/s43017-021-00199-z

Cameron, A. C., & Trivedi, P. K. (2013). *Regression analysis of count data*. Cambridge University Press.

Chen, M., Shi, W., Xie, P., Silva, V. B. S., Kousky, V. E., Wayne Higgins, R., & Janowiak, J. E. (2008). Assessing objective techniques for gauge-based analyses of global daily precipitation. *Journal of Geophysical Research: Atmospheres*, *113*(D4), https://doi.org/10.1029/2007JD009132

Chien, Y.-T., Wang, S.-Y. S., Chikamoto, Y., Voelker, S. L., Meyer, J. D. D., & Yoon, J.-H. (2019). North American winter dipole: Observed and simulated changes in circulations. *Atmosphere*, *10*(12), 793. https://doi.org/10.3390/atmos10120793

Cook, B. I., Ault, T. R., & Smerdon, J. E. (2015). Unprecedented 21st century drought risk in the American southwest and central plains. *Science Advances*, *1*(1), e1400082. https://doi.org/10.1126/sciadv.1400082

Cook, E. R., Woodhouse, C. A., Eakin, C. M., Meko, D. M., & Stahle, D. W. (2004). Long-term aridity changes in the western United States. *Science*, *306*(5698), 1015–1018. https://doi.org/10.1126/science.1102586

Delworth, T. L., Zeng, F., Rosati, A., Vecchi, G. A., & Wittenberg, A. T. (2015). A link between the Hiatus in global warming and North American drought. *Journal of Climate*, *28*(9), 3834–3845. https://doi.org/10.1175/jcli-d-14-00616.1

Deser, C., Phillips, A. S., Alexander, M. A., & Smoliak, B. V. (2014). Projecting North American climate over the Next 50 Years: Uncertainty due to internal variability. *Journal of Climate*, *27*(6), 2271–2296. https://doi.org/10.1175/jcli-d-13-00451.1

Diffenbaugh, N. S., Swain, D. L., & Touma, D. (2015). Anthropogenic warming has increased drought risk in California. *Proceedings of the National Academy of Sciences*, *112*(13), 3931–3936. https://doi.org/10.1073/pnas.1422385112

Eyring, V., Bony, S., Meehl, G. A., Senior, C. A., Stevens, B., Stouffer, R. J., & Taylor, K. E. (2016). Overview of the coupled model Intercomparison project phase 6 (CMIP6) experimental design and organization. *Geoscientific Model Development*, *9*(5), 1937–1958. https://doi.org/10.5194/gmd-9-1937-2016

Gelaro, R., McCarty, W., Suárez, M. J., Todling, R., Molod, A., Takacs, L., et al. (2017). The Modern-Era retrospective analysis for research and Applications, version 2 (MERRA-2). *Journal of Climate*, *30*(14), 5419–5454. https://doi.org/10.1175/jcli-d-16-0758.1

Gibson, P. B., Waliser, D. E., Guan, B., DeFlorio, M. J., Ralph, F. M., & Swain, D. L. (2020). Ridging associated with drought across the western and southwestern United States: Characteristics, trends, and predictability sources. *Journal of Climate*, *33*(7), 2485–2508. https://doi.org/10.1175/jcli-d-19-0439.1

Gillies, R. R., Wang, S.-Y., & Booth, M. R. (2010). Atmospheric scale interaction on wintertime intermountain west low-level inversions. *Weather and Forecasting*, *25*(4), 1196–1210. https://doi.org/10.1175/2010waf2222380.1

Hartmann, D. L. (2015). Pacific sea surface temperature and the winter of 2014. *Geophysical Research Letters*, *42*(6), 1894–1902. https://doi.org/10.1002/2015gl063083

Hersbach, H., Bell, B., Berrisford, P., Hirahara, S., Horányi, A., Muñoz-Sabater, J., et al. (2020). The ERA5 global reanalysis. *Quarterly Journal of the Royal Meteorological Society*, *146*(730), 1999–2049. https://doi.org/10.1002/qj.3803

Horton, D. E., Johnson, N. C., Singh, D., Swain, D. L., Rajaratnam, B., & Diffenbaugh, N. S. (2015). Contribution of changes in atmospheric circulation patterns to extreme temperature trends. *Nature*, *522*, 465–469. https://doi.org/10.1038/nature14550

Kalnay, E., Kanamitsu, M., Kistler, R., Collins, W., Deaven, D., Gandin, L., et al. (1996). The NCEP/NCAR 40-year reanalysis project. *Bulletin of the American Meteorological Society*, *77*(3), 437–471. https://doi.org/10.1175/1520-0477(1996)077<0437:tnyrp>2.0.co;2

Kay, J. E., Deser, C., Phillips, A., Mai, A., Hannay, C., Strand, G., et al. (2015). The community Earth system model (CESM) large ensemble project: A community resource for studying climate change in the presence of internal climate variability. *Bulletin of the American Meteorological Society*, *96*(8), 1333–1349. https://doi.org/10.1175/bams-d-13-00255.1

Kobayashi, S., Ota, Y., Harada, Y., Ebita, A., Moriya, M., Onoda, H., et al. (2015). The JRA-55 reanalysis: General specifications and basic characteristics. *Journal of the Meteorological Society of Japan. Ser. II*, *93*(1), 5–48. https://doi.org/10.2151/jmsj.2015-001

Lund, J., Medellin-Azuara, J., Durand, J., & Stone, K. (2018). Lessons from California's 2012–2016 drought. *Journal of Water Resources Planning and Management*, *144*(10), 04018067. https://doi.org/10.1061/(asce)wr.1943-5452.0000984

Mann, M. E., & Gleick, P. H. (2015). Climate change and California drought in the 21st century. *Proceedings of the National Academy of Sciences*, *112*(13), 3858–3859. https://doi.org/10.1073/pnas.1503667112

Piechota, T., Timilsena, J., Tootle, G., & Hidalgo, H. (2004). The western U.S. drought: How bad is it? *Eos, Transactions American Geophysical Union*, *85*(32), 301–304. https://doi.org/10.1029/2004eo320001

Robertson, A. W., & Ghil, M. (1999). Large-scale weather regimes and local climate over the western United States. *Journal of Climate*, *12*(6), 1796–1813. https://doi.org/10.1175/1520-0442(1999)012<1796:lswral>2.0.co;2

Rohde, R. A., Brillinger, D., Curry, J. A., Groom, D., Jacobsen, B., Muller, R. A., et al. (2011). The Berkeley Earth surface temperature averaging methodology. *AGU Fall Meeting Abstracts*, *43*, GC43B–0908.

Seager, R., Hoerling, M., Schubert, S., Wang, H., Lyon, B., Kumar, A., et al. (2015). Causes of the 2011–14 California drought. *Journal of Climate*, *28*(18), 6997–7024. https://doi.org/10.1175/jcli-d-14-00860.1

Singh, D., Swain, D. L., Mankin, J. S., Horton, D. E., Thomas, L. N., Rajaratnam, B., & Diffenbaugh, N. S. (2016). Recent amplification of the North American winter temperature dipole. *Journal of Geophysical Research: Atmospheres*, *121*(17), 9911–9928. https://doi.org/10.1002/2016jd025116

Stahle, D. W. (2020). Anthropogenic megadrought. *Science*, *368*(6488), 238–239. https://doi.org/10.1126/science.abb6902

Steinschneider, S., Ray, P., Rahat, S. H., & Kucharski, J. (2019). A weather-regime-based stochastic weather generator for climate vulnerability assessments of water systems in the western United States. *Water Resources Research*, *55*(8), 6923–6945. https://doi.org/10.1029/2018wr024446

Svoboda, M., LeComte, D., Hayes, M., Heim, R., Gleason, K., Angel, J., et al. (2002). The drought monitor. *Bulletin of the American Meteorological Society*, *83*(8), 1181–1190. https://doi.org/10.1175/1520-0477-83.8.1181

Swain, D., Tsiang, M., Haugen, M., Singh, D., Charland, A., Rajaratnam, B., & Diffenbaugh, N. (2014). The extraordinary California drought of 2013/2014: Character, context, and the role of climate change. *Bulletin of the American Meteorological Society*, *95*. S3–S7.

Swain, D. L. (2015). A tale of two California droughts: Lessons amidst record warmth and dryness in a region of complex physical and human geography. *Geophysical Research Letters*, *42*(22), 9999–10003. https://doi.org/10.1002/2015gl066628

Swain, D. L., Horton, D. E., Singh, D., & Diffenbaugh, N. S. (2016). Trends in atmospheric patterns conducive to seasonal precipitation and temperature extremes in California. *Science Advances*, *2*(4), e1501344. https://doi.org/10.1126/sciadv.1501344

Swain, D. L., Langenbrunner, B., Neelin, J. D., & Hall, A. (2018). Increasing precipitation volatility in twenty-first-century California. *Nature Climate Change*, *8*, 427–433. https://doi.org/10.1038/s41558-018-0140-y

Teng, H., & Branstator, G. (2017). Causes of extreme ridges that induce California droughts. *Journal of Climate*, *30*(4), 1477–1492. https://doi.org/10.1175/jcli-d-16-0524.1

Vigaud, N., Robertson, A. W., & Tippett, M. K. (2018). Predictability of recurrent weather regimes over North America during winter from submonthly reforecasts. *Monthly Weather Review*, *146*(8), 2559–2577. https://doi.org/10.1175/mwr-d-18-0058.1

Wang, S.-Y., Gillies, R. R., Martin, R., Davies, R. E., & Booth, M. R. (2012). Connecting subseasonal movements of the winter mean ridge in western North America to inversion climatology in cache valley, Utah. *Journal of Applied Meteorology and Climatology*, *51*(3), 617–627. https://doi.org/10.1175/jamc-d-11-0101.1

Wang, S.-Y., Hipps, L., Gillies, R. R., & Yoon, J.-H. (2014). Probable causes of the abnormal ridge accompanying the 2013–2014 California drought: ENSO precursor and anthropogenic warming footprint. *Geophysical Research Letters*, *41*(9), 3220–3226. https://doi.org/10.1002/2014gl059748

Wang, S.-Y., Yoon, J.-H., Becker, E., & Gillies, R. (2017). California from drought to deluge. *Nature Climate Change*, *7*(7), 465–468. https://doi.org/10.1038/nclimate3330

Williams, A. P., Cook, E. R., Smerdon, J. E., Cook, B. I., Abatzoglou, J. T., Bolles, K., et al. (2020). Large contribution from anthropogenic warming to an emerging North American megadrought. *Science*, *368*(6488), 314–318. https://doi.org/10.1126/science.aaz9600

Williams, A. P., Seager, R., Abatzoglou, J. T., Cook, B. I., Smerdon, J. E., & Cook, E. R. (2015). Contribution of anthropogenic warming to California drought during 2012–2014. *Geophysical Research Letters*, *42*(16), 6819–6828. https://doi.org/10.1002/2015gl064924

Xie, S.-P., Deser, C., Vecchi, G. A., Ma, J., Teng, H., & Wittenberg, A. T. (2010). Global warming pattern formation: Sea surface temperature and rainfall. *Journal of Climate*, *23*(4), 966–986. https://doi.org/10.1175/2009jcli3329.1

Yoon, J.-H., Wang, S.-Y. S., Gillies, R. R., Kravitz, B., Hipps, L., & Rasch, P. J. (2015). Increasing water cycle extremes in California and in relation to ENSO cycle under global warming. *Nature Communications*, *6*(1), 8657. https://doi.org/10.1038/ncomms9657

Zhang, W., & Villarini, G. (2019). On the weather types that shape the precipitation patterns across the U.S. Midwest. *Climate Dynamics*, *53*(7), 4217–4232. https://doi.org/10.1007/s00382-019-04783-4

19448007, 2022, 1, Downloaded from https://agupubs.onlinelibrary.wiley.com/doi/10.1029/2021GL097089 by Office Of Scientific And Technical Information, Wiley Online Library on [28/07/2023]. See the Terms and Conditions (https://onlinelibrary.wiley.com/terms-and-conditions) on Wiley Online Library for rules of use; OA articles are governed by the applicable Creative Commons License

Zhang, W., & Villarini, G. (2021). Greenhouse gases drove the increasing trends in spring precipitation across the central USA. *Philosophical Transactions of the Royal Society A: Mathematical, Physical & Engineering Sciences*, *379*(2195), 20190553. https://doi.org/10.1098/rsta.2019.0553

Reference From the Supporting Information

Likas, A., Vlassis, N., & Verbeek, J. J. (2003). The global k-means clustering algorithm. *Pattern Recognition*, *36*(2), 451–461. https://doi.org/10.1016/s0031-3203(02)00060-2

19448007, 2022, 1, Downloaded from https://agupubs.onlinelibrary.wiley.com/doi/10.1029/2021GL097089 by Office Of Scientific And Technical Information, Wiley Online Library on [28/07/2023]. See the Terms and Conditions (https://onlinelibrary.wiley.com/terms-and-conditions) on Wiley Online Library for rules of use; OA articles are governed by the applicable Creative Commons License